

PRODUCTION AND PHENOMENOLOGY OF GLUEBALLS\*

BNL--42223

Chang S. Chan  
City College of New York

DE89 009529

and

S.J. Lindenbaum  
Brookhaven National Laboratory  
and  
City College of New York

(Presented by: Chang S. Chan)

Paper presented at "Excited Baryons - 1988"  
Rensselaer Polytechnic Institute  
Troy, New York  
August 4-6, 1988

November 28, 1988

**DISCLAIMER**

This report was prepared as an account of work sponsored by an agency of the United States Government. Neither the United States Government nor any agency thereof, nor any of their employees, makes any warranty, express or implied, or assumes any legal liability or responsibility for the accuracy, completeness, or usefulness of any information, apparatus, product, or process disclosed, or represents that its use would not infringe privately owned rights. Reference herein to any specific commercial product, process, or service by trade name, trademark, manufacturer, or otherwise does not necessarily constitute or imply its endorsement, recommendation, or favoring by the United States Government or any agency thereof. The views and opinions of authors expressed herein do not necessarily state or reflect those of the United States Government or any agency thereof.

MASTER

\* Research carried out under the auspices of the U.S. Department of Energy under Contract Nos. DE-AC02-76CH00016 (BNL) and DE-AC02-83ER40107 (CCNY).

# PRODUCTION AND PHENOMENOLOGY OF GLUEBALLS\*

Chang S. Chan  
City College of New York

and

S.J. Lindenbaum  
Brookhaven National Laboratory  
and  
City College of New York

(Presented by: Chang S. Chan)

## ABSTRACT

After a brief introduction, the current status of the prominent glueball candidates are reviewed. In particular, we present a partial wave analysis of 6658 events of the reaction  $\pi^-p \rightarrow \phi\eta\eta$  at 22 GeV/c. The data analysis reveals three resonances  $g_T(2010)$ ,  $g_T'(2300)$  and  $g_T''(2340)$ , all with the same quantum numbers  $I^{GJPC} = 0^+2^{++}$  which comprise virtually all the production cross section. The large  $\phi\eta\eta$  signal occurs over a mostly structureless and incoherent  $\phi K^+K^-$  background. The absence of the expected OZI suppression, and the striking differences of these states from conventional states and background in other channels has so far only been successfully explained by assuming they are produced by 1-3  $JPC = 2^{++}$  glueballs (multigluon resonances). The forthcoming search for an exotic  $JPC$  glueball is also discussed.

---

\* Research carried out under the auspices of the U.S. Department of Energy under Contract Nos. DE-AC02-76CH00016 (BNL) and DE-AC02-83ER40107 (CCNY).

## INTRODUCTION

Quantum Chromodynamics (QCD) the current theory of hadronic forces has quarks interacting through the exchange of the vector gauge bosons called gluons. In this theory, quarks carry a color charge that may take one of three values.

The heart of QCD is the locally gauge invariant non-Abelian group  $SU(3)_{\text{color}}$  which has eight colored massless gauge bosons, which self-interact. Their interaction exhibits asymptotic freedom and is described by a running coupling constant. The effective experimental values of  $\Lambda$  are of the order of 100 MeV. Thus asymptotic freedom\* is quite "precocious" even at moderate  $q^2$  and energies. Color is confined, thus hadronic states that are not color singlets are unobservable.

The self-interaction of the gauge bosons which occurs in non-Abelian gauge theory (gluons in QCD) but not in Abelian gauge theory (photons in QED) is a most characteristic feature of QCD. Color confinement and the running coupling constant make the existence of multi-gluon resonances or glueballs inescapable.<sup>1)</sup> This has been quantitatively demonstrated by Lattice Gauge calculations.<sup>2)</sup> In a pure Yang-Mills theory of  $SU(3)$  color, glueballs would be the only hadrons in the world.

If at least one glueball is not established in our opinion the validity of QCD in the strong coupling non-perturbative region would be in serious question. Experimental evidence for glueball candidates has been presented by various groups at the Munich Conference.<sup>3)</sup> In particular, the BNL/CCNY collaboration<sup>4)</sup> has discovered three  $I^{GJPC} = 0^{+2++}$  states ( $g_T$ ,  $g_{T1}$ ,  $g_{T''}$ ). The very striking and unusual characteristics of the data have found a natural glueball explanation for these states within the context of QCD whereas alternative explanations have been shown to be incorrect, do not fit the data, or

---

\* The effective strong coupling decreases asymptotically as the momentum transfer (or interaction energy) increases.

both.<sup>5)</sup> Thus these states constitute the strongest glueball candidates, and are very probably produced by at least 1 primary  $J^{PC} = 2^{++}$  glueball. Therefore a primary objective of this paper is to focus our attention on this channel for glueball search and to present the detailed description of the analysis.

## GLUEBALL PRODUCTION

Glueballs are isosinglets since gluons carry no isospin or electric charge. Two-gluon states are required to have even C-parity while three-gluon states are allowed to have either odd or even C-parity depending upon whether the SU(3) coupling is symmetric or antisymmetric.

Experimentally, the detection of glueballs is complicated by the predominance of  $q\bar{q}$  states.

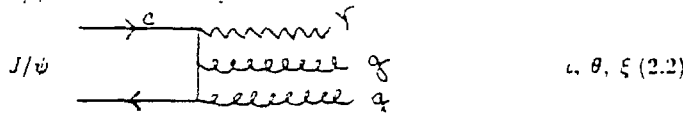
It appears from LGT calculations that the lowest lying glueballs are  $0^{++}$  and  $2^{++}$ . The best estimates of the  $0^{++}$  ground state mass are in the range  $\sim 1.0 - 1.5$  GeV. The  $2^{++}$  glueball mass is estimated to be  $> 1.5$  GeV and probably  $\sim 2$  GeV. Due to insufficient lattice size due to lack of sufficient computer power, these present estimates are to be used only as a guide. However the three masses of the  $g_T$ 's seem to be reasonable for  $2^{++}$  glueballs.

From the success of the quark model it is obvious that the  $q\bar{q}$  and  $qq\bar{q}$  states dominate the hadronic sector and in particular these states cover the region 1-2.5 GeV where glueballs are most likely to be produced. It is expected that low-lying glueballs are masked in the quark-built meson nonets which makes the unambiguous identification of glueballs difficult.

There are four general methods of searching for glueballs. These are listed below and shown in Fig. 1. The prominent glueball candidates are shown in brackets.

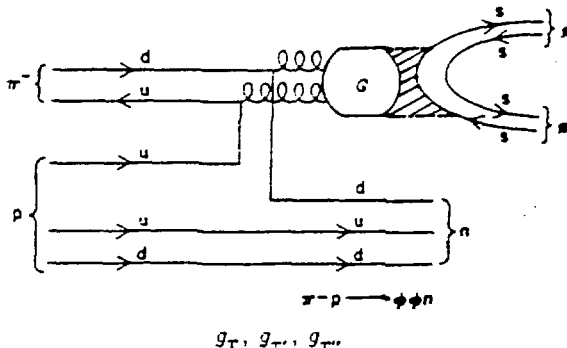
1.  $J/\psi$  radiative decay [iota,  $\theta$ ,  $\xi(2.2)$ ]. Although it was hoped this channel would be an efficient glueball channel, it sees mainly conventional  $q\bar{q}$  states and continuum and thus is at best a very inefficient glueball filter. .

1.  $J/\psi$  Radiative Decay



$\iota, \theta, \xi$  (2.2)

2. OZI Violating



3. Hadronic interaction pattern recognition of extra isosinglet states in addition to  $q\bar{q}$  nonets  $\iota, G, S^*, g_s$ .

4. Double Pomeron Exchange

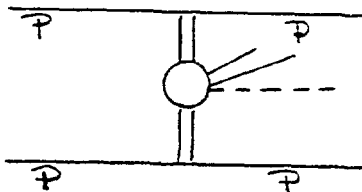


Figure 1

2. OZI violating [ $g_T, g_{T'}, g_{T''}$ ]. As we shall discuss later this method which was the first to obtain strong evidence for glueballs has turned out to be the tightest glueball filter which highly rejects conventional  $q\bar{q}$  states and easily passes resonating glue states such as glueballs and thus has the strongest evidence for glueballs.

3. Hadronic interaction pattern recognition of extra isosinglet states in addition to  $q\bar{q}$  nonets, iota,  $G, S^*, g_s$ . This method has no filtering action but searches for extra isosinglet states. It appears that especially in the  $0^-+$  channel there may be

one too many isoscalars to be easily accommodated as  $q\bar{q}$ . If that turns out to be the case this extra isosinglet could be due to a glueball, a multiquark state, or a hybrid (i.e.  $qqg$ ) and the identification of a glueball would be very difficult.

#### Iota(1460) [ $\eta(1460)$ ] Related Work

Cason et al., Paper 235C (Munich Conference), Notre Dame/Brandeis/BNL/CCNY/Duke, studied 21.4 GeV/c  $\pi^-p \rightarrow K_s^0 K_s^0 \pi^0 n$ . A reaction for which  $C = +1$  only. In contrast to similar experiments at lower energy where  $C = \pm 1$  that their mass spectrum resembled that of the iota in the region of 1460. A fit to the mass spectrum and partial wave analysis with a  $|t'| > 0.3$  cut revealed evidence for a  $JPC = 0^{-+}$  resonance with  $M = 1453 \pm 7$ ,  $\Gamma = 100 \pm 11$  while  $1^{++}$  was structureless. The  $0^{-+}$   $\eta(1420)$  appeared suppressed but consistent with other results (Fig. 2).

Paper 386, Ando et al. (Munich Conference), Sugiyama/Nagoya/KEK/Kyoto/Miyazaki/Nagoya Med. Tech./Kyoto U. of Ed., found that 8.06  $\pi^-p \rightarrow K_s^{\pm} K_s^{\mp} \pi^0 n$  gave mass spectrum and partial wave analysis results consistent with a  $0^{-+}$   $\eta(1420)$  at  $M = 1424$  MeV and  $\Gamma = 35$  MeV. A hint of an  $\eta(1280)$  was also observed.

In Paper 595c (Munich Conference), Fukui et al., Sugiyama/Nagoya/KEK/Kyoto/Miyazaki/Nagoya Med. Tech./Kyoto U. of Ed., both the  $0^{-+}$   $\eta(1275)$  and  $\eta(1420)$  were clearly observed in the  $\eta\pi^+\pi^-$  system (Fig. 3).

Birman et al., (paper 657, Munich Conference) performed a high statistics partial wave analysis of the  $K^+K^- \pi^-$  system produced by 8 GeV/c  $\pi^-$ . They found a complicated situation which needed many waves to fit, clearly showing that high statistics partial wave analyses are needed to draw critical conclusions.

They found at least one  $0^{-+}$  near 1.4 GeV or perhaps 2 resonances between 1.4-1.5 GeV, and an indication of a  $0^{-+}$  resonance at 1.28 GeV.

The SLAC iota(1460) has an asymmetrical shape which when analyzed also suggests more than one resonance in that region. Since only two  $0^{-+}$  resonances can be naturally accommodated as first  $q\bar{q}$  radial

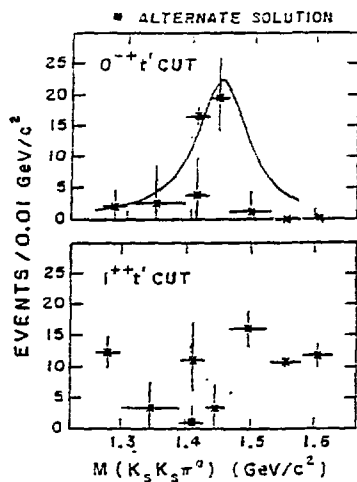


Fig. 2  $\pi^- p \rightarrow K_s^0 K_s^0 \pi^0 \eta$

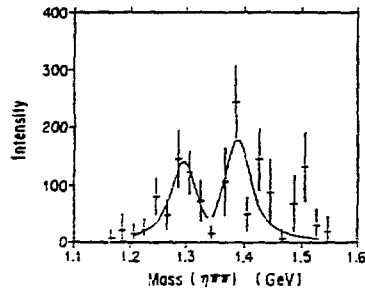


Fig. 3  $n(1275)$  and  $n(1420)$

excitations it is important to determine whether there is a third, which then could be a candidate for a glueball, multiquark or hybrid state. The complications due to the vacuum and its possible effects on the mass of higher radial excitations must also be considered in the  $0^-+$  spectroscopy.

#### $\theta(1720)$ [ $f_2(1720)$ ] Related Work

Paper A498 (Munich Conference), B. Ratcliff *et al.*, (LASS), found in the experiment  $K^- p \rightarrow K_s^0 K_s^0 \Lambda$  that while they clearly saw the  $f'$  peak there was no evidence for the  $\theta^6)$  (see Fig. 4a) although this was expected from a prior coupled channel analysis.<sup>7)</sup> This led Lindenbaum and Longacre to request from MK III the latest information on the status of the  $\theta$  quantum numbers. The Bolton Thesis<sup>8)</sup> which Walter Toki sent us made it clear that one could not distinguish between  $0^{++}$  and  $2^{++}$  or a mixture for the  $\theta$  quantum numbers.

If the  $\theta$  was  $0^{++}$  then it would have the same mass width and quantum numbers of the  $S^*$  (within the errors)<sup>9</sup> discovered prior to the  $\theta$ . In the scenario where the  $S^*$  and  $\theta$  are the same particle this modification of the coupled channel analysis was then found consistent<sup>3)</sup> with the LASS data (Fig. 4b).

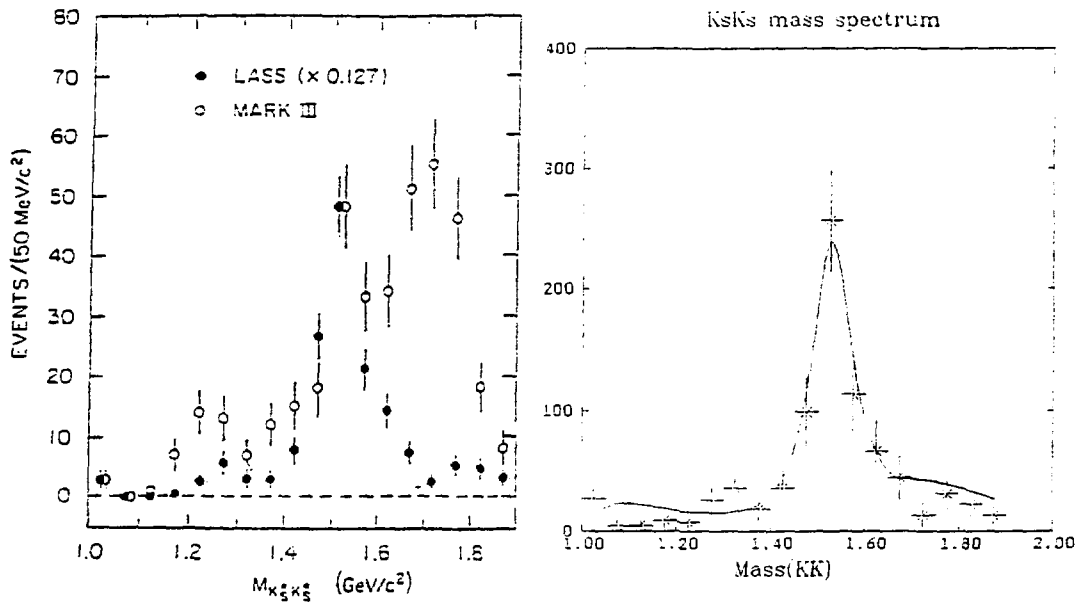


Fig. 4a The comparison of the  $K^0\bar{K}^0$  mass distribution from LASS and MK III with that from radiative  $J/\psi$  decay from threshold up to  $1.9\text{ GeV}/c^2$

Figure 4b

Furthermore it should be noted that if the  $\theta$  has  $0^{++}$  and is assumed to be the same as the  $S^{\ast}$ , the status of the  $G(1590)$  comes into question since the  $G(1590)$  used an  $\epsilon(-1230 \pm 30)$  in its fitting whereas all other analyses used an  $\epsilon(-1450)$ . Lindenbaum and Longacre<sup>3,11</sup> have using the usual criterion of fitting the data with a minimum number of resonances found that the  $0^{++}$   $S^{\ast}$ ,  $g_S$ ,  $\epsilon$  and  $S^{\ast}$  fit the data reasonably, some of which is shown in Figs. 4b-d. Whereas the  $S^{\ast}$ ,  $G$ ,  $\epsilon$  and  $S^{\ast}$  do not fit the data.

Further work on this preliminary analysis is still in progress. DM2 does not see the narrow SLAC  $\xi$  but instead a broad enhancement.

LASS finds in the  $\xi(2200)$  region a state which is likely  $s\bar{s}$  and has  $J^{PC} = 4^{++}$  or perhaps  $2^{++}$  and could have a width which ranges from substantial to narrow. Thus the  $\xi$  does not appear to be a glueball candidate and instead appears to be an  $s\bar{s}$  quark state.

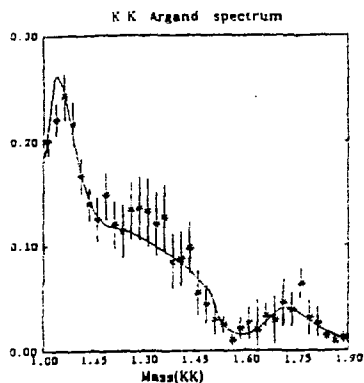


Fig. 4c Fit (Lindenbaum and Longacre) to  $K\bar{K}$  mass spectrum with  $\theta = S^*$

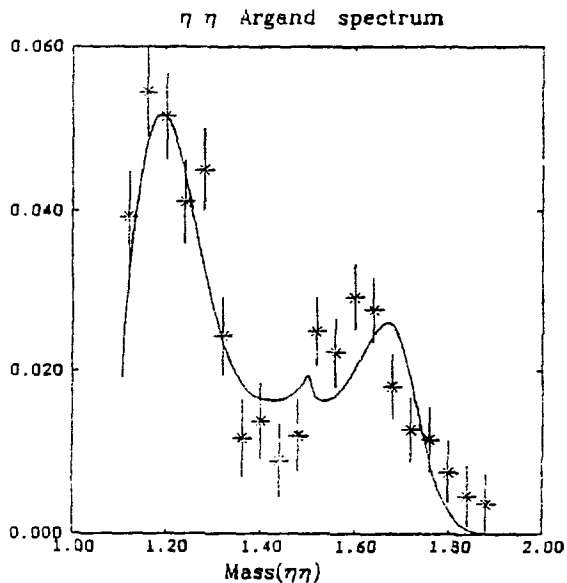


Fig. 4d Fit (Lindenbaum and Longacre) to  $\eta\eta$  mass spectrum with  $\theta = S^*$

### Double Pomeron Exchange

Paper 521 (Munich Conference), Palano et al., Athens/Bari/Birmingham/CERN/College de France/LPNHE observed high statistics centrally produced  $\pi^+\pi^-$  in the reaction 300 GeV/c  $p + p \rightarrow p(\pi^+\pi^-)p$ . They found the main features of the  $S^*$  drop at  $K\bar{K}$  (Fig. 5) threshold best described as interference of the  $S^*$  with background. This explanation should also apply to this striking phenomenon previously observed at ISR. DPE seems to be a good  $0^{++}$  selector but not likely an efficient glueball filter.

### Other $\phi\phi$ Experiments

Booth et al.,<sup>12)</sup> conclude the  $\phi\phi$  is mainly  $2^{++}$  and are consistent with  $g_T'$  and  $g_T''$ . They do not expect to see  $g_T$  due to acceptance.

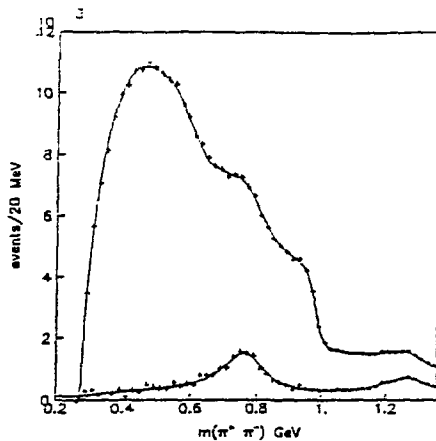


Fig. 5 300 GeV/c  $p + p$  central production of  $\pi^+ \pi^-$

Mark III in  $J/\psi \rightarrow \gamma\phi\phi$  found  $\approx$  few hundred events. They are  $\approx$  75%  $0^{-+}$  with very little  $2^{++}$  in the remainder. Since  $J/\psi$  radiative decay mainly sees  $0^{-+}$  and is obviously an inefficient glueball filter since it sees mainly conventional objects such as  $n$ ,  $n'$ ,  $f$ ,  $f'$  etc. and continuum, it is not surprising they do not see  $g_T$ ,  $g_{T'}$  and  $g_{T''}$  with their very low statistics  $\phi\phi$ . Secondly the width of the  $J/\psi + ggg$  and the branching ratio to radiative decay agrees with perturbative calculations. Therefore if  $J/\psi$  radiative decay were strongly coupled to glueballs one might expect that the process  $J/\psi + \gamma G$  would enhance the  $J/\psi$  radiative decay branching ratio and in the process increase the width of the  $J/\psi$ . In contrast in  $\pi^- p \rightarrow \phi\phi n$ , only the  $g_T$ 's are seen and no conventional objects or continuum appears. Not even a trace of the  $4^{++} h(2030)$  is seen even though we can easily detect it with the enormous analysis power of the  $\phi\phi$  system. Thus there are huge factors in the filter action for glueballs in favor of the  $\pi^- p \rightarrow \phi\phi n$  channel. Furthermore BNL/CCNY do not see  $0^{-+}$  since  $\pi$ -exchange observes only  $0^{++}$ ,  $2^{++}$ ,  $4^{++}$  etc. Thus we see no inconsistency between BNL/CCNY and MK III.

## THE OZI RULE AS A GLUEBALL FILTER IN DISCONNECTED ZWEIG DIAGRAMS

In order to disentangle glueballs from quark-built meson nonets it is essential that a special selection rule or filtering process be used.  $J/\psi$  radiative decay, which has been considered to be a promising place to look for glueballs, is in effect not an efficient glueball filter since, in addition to uncovering glueball candidates such as iota and  $\theta$ , many conventional states like  $f$ ,  $f'$ ,  $n$  and  $n'$  etc. have also been identified in this decay mode. It turns out that the striking observations of the complete breakdown of OZI suppression in the production of two phi-mesons in non-strange hadronic interactions as well as the unusual characteristics of the data can be well explained by the OZI rule playing the role of an efficient glueball filter.

It has been established experimentally and phenomenologically that in the light quark ( $u, d, s$ ) sector, except for the  $JPC = 0^{-+}$  nonet, which is subject to vacuum mixing, other established  $1^{--}$ ,  $2^{++}$  and  $3^{--}$  nonets<sup>13)</sup> are nearly ideally mixed. An ideally mixed nonet can be conveniently displayed by Zweig's Quark Line Diagrams. In this picture, hadronic reactions are depicted by the behavior of the individual quarks that make them up. A reaction which proceeds by a continuous flow of quark lines carrying color from the initial state to a final state hadron or hadrons is considered an OZI allowed process (Fig. 6). In QCD, an allowed process is characterized by a series of single gluon exchange which involve strong collective soft glue effects to create or annihilate  $q\bar{q}$  pairs relatively easily. In contrast, reactions in which the quark lines are disconnected are considered forbidden (Fig. 7). From the QCD point of view the disconnection of the topological flow of quark lines in a forbidden process is bridged by the exchange of a pure gluonic system made up by two or three hard gluons. Vector mesons like  $\phi$  and  $J/\psi$  require three hard gluons in the exchange process while tensor mesons like  $f'$  require only two hard gluons. Even at moderate gluon energies, as seen in the decay of  $\phi$ , the precocious asymptotic freedom strongly decouples quarks from gluons. Thus, the resultant relatively weak coupling constants of the hard gluons naturally explains the OZI

CONNECTED  
ALLOWED PROCESS

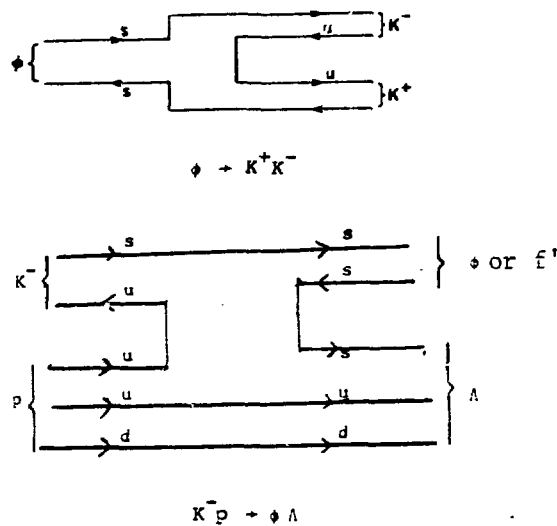


Fig. 6 Zweig connected (allowed reaction) diagrams for the  $u, d, s$  quark system.

DISCONNECTED  
FORBIDDEN (SUPPRESSED)

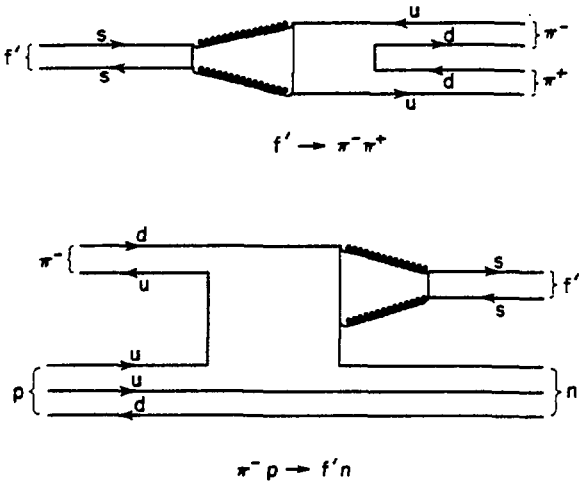


Figure 7

suppression in the disconnected diagrams or equivalently, ideal mixing for meson systems of spin greater than zero. For spin zero systems vacuum mixing effects<sup>22)</sup> can badly distort the associated nonet so that it is far from ideally mixed. In QCD, the only other basic mixing mechanism is due to the intervention of a glueball. This glueball mixing mechanism would lead to a breakdown of the OZI suppression. A glueball resonance is expected to be relatively strongly coupled.

The OZI rule works extremely well in predicting the narrowness of  $J/\psi$  or  $T$  which is assumed to be a nearly pure  $c\bar{c}$  or  $b\bar{b}$  state, respectively with no open decay channels containing charmed or bottom quarks.  $\phi$  and  $f'$  are generally considered to be almost pure strangeonium states. The observed small branching ratios of  $\phi$  and  $f'$  decaying into pions relative to kaons are consistent with the expected suppression arising from the disconnected quark lines compared to the connected ones. Experimentally, the OZI suppression factors have been measured to be typically of  $\sim 100$ . For example, comparisons of production for both  $\phi$  and  $f'$  in allowed and forbidden channels are experimentally found to be

$$\frac{\sigma(K^-p \rightarrow \phi\Lambda)}{\sigma(\pi^-p \rightarrow \phi n)} \sim 60 \quad (1)$$

$$\frac{\sigma(K^-p \rightarrow f'\Lambda)}{\sigma(\pi^-p \rightarrow f'n)} \sim 50 \quad (2)$$

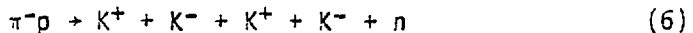
However, similar reactions for production of the  $\phi\phi$  system<sup>14,15)</sup> showed that the ratio of production cross sections for the allowed to the forbidden processes is within a factor of -3:

$$\frac{\sigma(K^-p \rightarrow \phi\phi\Lambda/\Sigma^0)}{\sigma(\pi^-p \rightarrow \phi\phi n)} \sim 3 \quad (3)$$

It is evident that the expected OZI suppression is virtually absent in the supposedly suppressed channel

$$\pi^-p \rightarrow \phi + \phi + n \quad (4)$$

To see how badly the OZI rule is violated in this forbidden channel, it is instructive to compare reaction (4) to two other companion reactions which are allowed by the OZI rule:



All of these three reactions (4), (5) and (6), studied by the BNL/CCNY group in four generations of experiments since 1978<sup>4)</sup> were measured in the same experiment since the  $\phi$  mesons from reaction (4) were detected by the kaons from the decay  $\phi \rightarrow K^+ + K^-$  and thus the actual final reaction we measured was reaction (6).

The Quark Line Diagrams for reactions (4), (5) and (6) are shown in Figs. 8a-d. All of the events corresponding to reaction (6) were used in the scatter plot (Fig. 9) in which the effective mass of a pair of  $K^+K^-$  is plotted against the mass of the other  $K^+K^-$  pair. Since the correct association of  $K^+K^-$  pair is not known, two mass combinations are plotted for each event. It is clear that two narrow bands corresponding to  $\phi$  mesons are easily identifiable. The black spot at the overlap of the two  $\phi$  bands is an obvious indication of a huge  $\phi\phi$  signal where very little was expected. After correcting for double counting and resolution, it is found that the density of  $\phi\phi$  events [Reaction (4)] towers over that of  $K^+K^-K^+K^-$  events [Reaction (6)] by a factor of 1000, and over that of  $\phi K^+K^-$  events [Reaction (5)] by a factor of 50. Note that even after a wide cut ( $\pm 14$  MeV) for  $\phi$

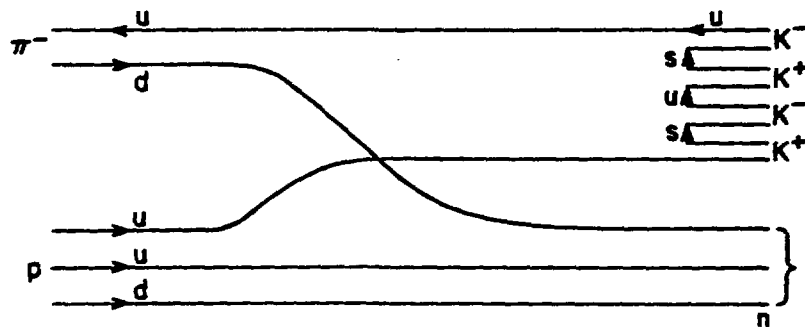


Fig. 8a The Zweig Quark Line Diagram for the reaction  $\pi^- p \rightarrow K^+ K^- K^+ K^- n$ , which is connected and OZI allowed.

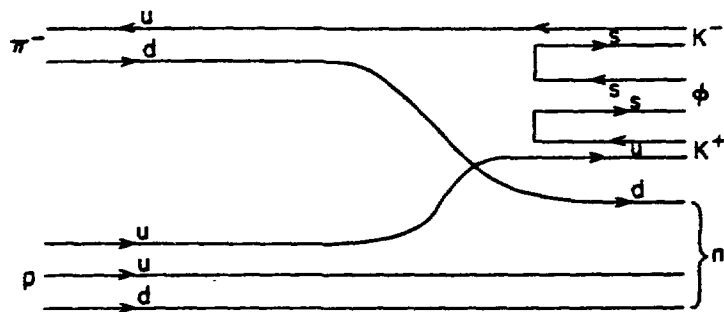


Fig. 8b The Zweig Quark Line Diagram for the reaction  $\pi^-p \rightarrow \phi K^+ K^- n$ , which is connected and OZI allowed.

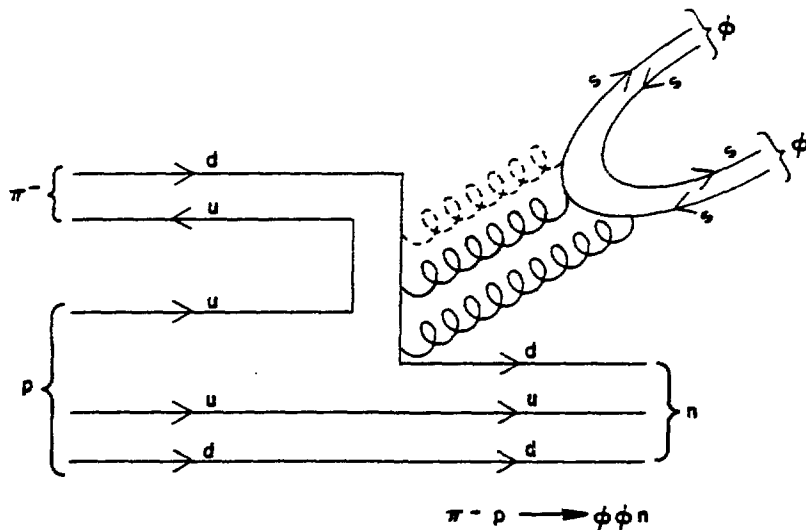


Fig. 8c The Zweig Quark Line Diagram for the reaction  $\pi^-p \rightarrow \phi\phi n$ , which is disconnected (i.e., a double hairpin diagram) and is OZI forbidden. Two or three gluons are shown connecting the disconnected parts of the diagram depending upon the quantum numbers of the  $\phi\phi$  system. For the  $g_T$ 's,  $JPC = 2^{++}$  and only two gluons are required. From the data analysis, they come from the annihilation of the incident  $\pi^-$  and a  $\pi^+$  exchanged between the lower and the upper parts of the diagram.

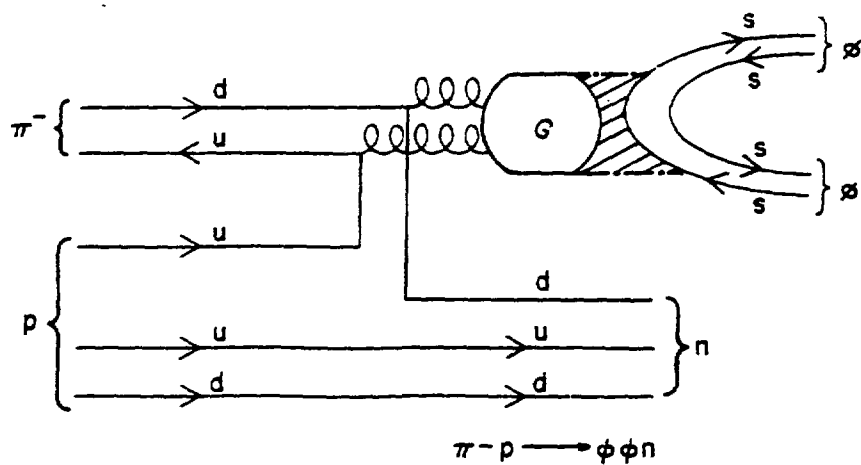


Fig. 8d The  $J^{PC} = 2^{++}$  glueball intermediate state in  $\pi^- p \rightarrow \phi\phi n$ . The region of crosshatched lines within the dash-dot lines indicates that we do not know the details of the glueball hadronization into  $\phi\phi$ .

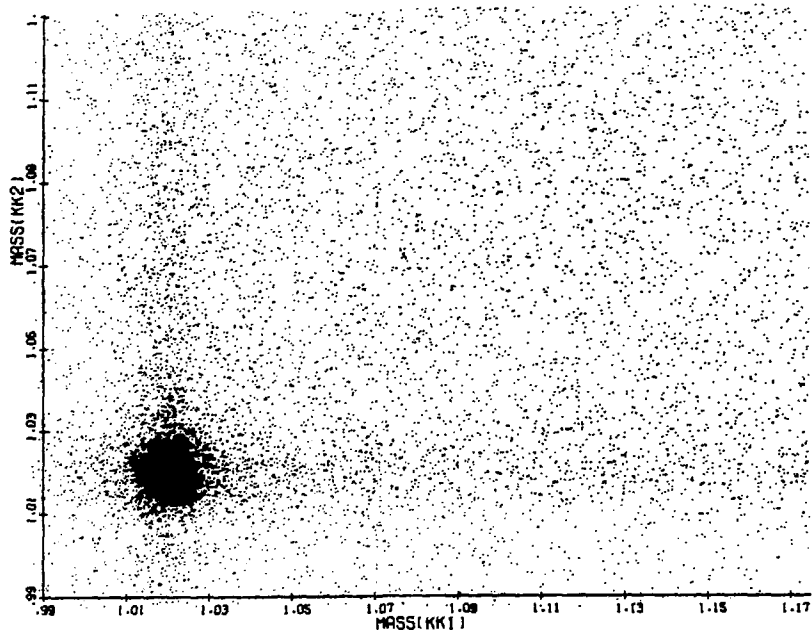


Fig. 9 Scatterplot of  $K^+K^-$  effective mass for each pair of  $K^+K^-$  masses. Clear bands of  $\phi(1020)$  are seen with an enormous enhancement (black spot) where they overlap (i.e.,  $\phi\phi$ ). This overlap essentially represents a complete breakdown of OZI suppression.

(1019 MeV), our  $\phi\phi$  data is still about 10 times more than the background  $\phi K^+K^-$  events from Reaction (5). The vector nature of  $\phi$ , accompanied by the high statistics  $\phi\phi$  data sample (6658 events) above the relatively low background level (13%), make our partial wave analysis remarkably powerful. Indeed, the final solution of a set of three  $2^{++}$  waves which was sought among a vast number of partial waves (114  $\phi\phi$  waves) is distinctly selective and unique.

It is apparent that based on these experimental facts the OZI rule is completely broken in the reaction  $\pi^-p \rightarrow \phi\phi n$ . A quantitative treatment<sup>16)</sup> of these reactions led to the same conclusion. Results of our partial wave analysis show that the  $\phi\phi$  data requires three resonances all with  $J^{PC} = 2^{++}$  which is known to be ideally mixed even in its first radial excitation. This certainly rules out the possibility of a vacuum mixing. Thus breakdown of the OZI rule seen in Reaction (4) can only be attributed to the other basic flavor mixing mechanism in QCD, namely the intervention of glueballs which destroys the ideal mixing. The fact that there is no indication of  $h(2040)$  ( $I^{GJPC} = 0^+4^{++}$ ), which is also produced by  $\pi$ -exchange, in the  $\phi\phi$  data shows how well the filtering action is working in this channel.

#### PARTIAL WAVE ANALYSIS

We have obtained 6658  $\phi\phi$  events, each with an identified neutron. After a missing mass squared cut ( $MM^2 < 1.6$  GeV<sup>2</sup>) for the recoil neutron the estimated background is less than 5% which should have a negligible effect on our partial wave analysis. The  $\phi\phi$  system final state is a four-body system in which each  $\phi$  is a vector and its helicity structure is transmitted to the decay products  $K^+K^-$ . Thus the  $\phi\phi$  system has excellent analyzing power due to the vector nature of  $\phi$ , its narrowness and the identity of its two constituent  $\phi$ 's. This system is constrained by both Bose and Charge symmetries. Thus isospin  $I = 0$ , total  $\phi\phi$  spin  $S = 0, 1, 2$ ,  $L + S$  must be even, and C-parity is plus.

The standard LBL/SLAC isobar model P.W.A. program was used but modified so that the spectator particle was replaced by a decaying  $\phi$ . Due to the narrowness of the  $\phi$  (less than the experimental resolution  $\Gamma_{\phi\phi} 8$  MeV), the analysis was independent of the isobar assumption and depended on the angular characteristics of the partial waves. The decay of the  $\phi\phi$  system was characterized by six-angles, the usual Gottfried-Jackson and Trieman-Yang angles ( $\beta, \gamma$ ) in the  $\phi\phi$  CMS rest frame (Fig. 10a), and the polar ( $\theta_1, \theta_2$ ) and azimuthal ( $\alpha_1, \alpha_2$ ) decay angles of each  $\phi$  in its own rest frame (Fig. 10b).

The angular dependence of the physical quantities and fitting parameters of interest such as the differential cross section and likelihood function can be expressed in terms of a basis vector. Each basis vector  $G(\beta, \gamma, \theta_1, \theta_2, \alpha_1, \alpha_2)$  is designated by a set of six quantum numbers  $J^P L S M \eta$  and has the explicit form:

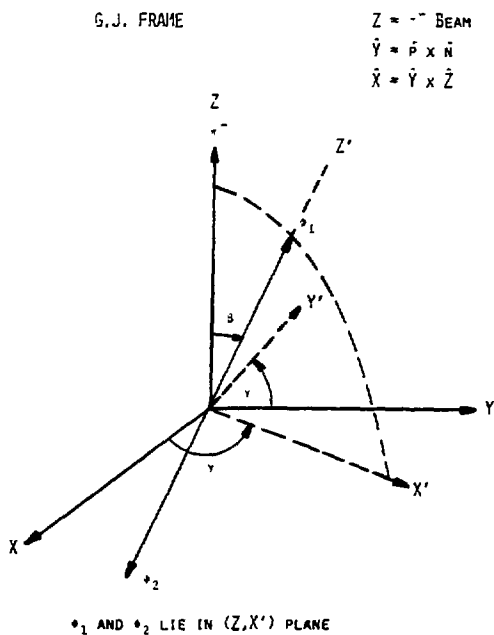


Fig. 10a The Gottfried-Jackson frame with polar angle  $\beta$  and azimuthal angle  $\gamma$ .

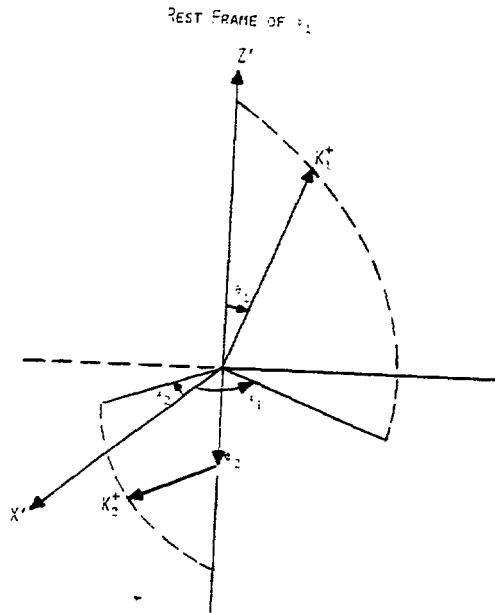


Fig. 10b The  $\phi_1$  rest frame with the polar angle  $\theta_1$  of the decay  $K_1^+$  (relative to  $\phi$  direction) and the azimuthal angle  $\alpha_1$  of the decay  $K_1^+$ .

$$\begin{aligned}
 G^{J^P LSM^n} (\beta, \gamma, \theta_1, \theta_2, \alpha_1, \alpha_2) = \\
 \text{Real} \left[ \frac{(1+i) - n(1+i)}{2} \sum_{\mu, \lambda} C(1, 1, S/\mu, -\lambda) C(L, S, J/0, \mu - \lambda) \right. \\
 \left. e^{-iM\gamma} e^{i\mu\alpha_1} e^{i\lambda\alpha_2} d_{M, \mu - \lambda}^J(\beta) d_{\mu, 0}^1(\theta_1) d_{\lambda, 0}^1(\theta_2) \right] \quad (7)
 \end{aligned}$$

where  $\mu, \lambda$  = helicities of the  $\phi$ 's (-1, 0, 1)

$C$  = Clebsch-Gordon coefficients.

$n$  = -1 (unnatural) or +1 (natural)

The complete set of the basis vectors can be used to determine the relative amounts of the partial waves associated with the basis vectors in describing the experimentally measured angular distributions. The differential cross section is given by

$$\frac{dI(\Omega)}{d\Omega} = \left| \sum_{J^P LSM^n} A_{J^P LSM^n} * G^{J^P LSM^n}(\Omega) \right|^2 \quad (8)$$

where  $\Omega = (\beta, \gamma, \theta_1, \theta_2, \alpha_1, \alpha_2)$  and  $A_j P_{LSM}^n$  is a fitting parameter to be determined by maximizing the likelihood function defined by events

$$\log L = \sum_{i=1} \log I(\Omega_i) - \sum_{j,k} A_j M_{j,k} A_k \quad (j,k = j^P_{LSM} \eta) \quad (9)$$

The  $M_{j,k}$  is an acceptance matrix which is an essential ingredient in determining the fitting parameters  $A_j$ . We determined the acceptance by a Monte Carlo program which took into account the geometry of our apparatus, multiple scattering, kaon decay, detector inefficiencies, pattern recognition inefficiencies, and the various cuts used in the analysis. We calculated a precise six-dimensional differential acceptance  $a(\Omega)$  for each mass of 10 MeV width which was comparable to our experimental resolution  $\Gamma_{\phi\phi} \sim 8$  MeV. This differential acceptance was integrated over each partial wave and all the interference between them, thus forming an acceptance matrix  $M$ :

$$M_{j,k} = \int G_j G_k a(\Omega) d\Omega \quad (10)$$

Figure 11a shows the acceptance and the acceptance corrected  $\phi\phi$  mass spectrum (2.04 - 2.64 GeV) in the ten mass bins mostly 50 MeV wide except near the ends. Nearly 30% of the events have been removed from the 75 MeV threshold bin (2.040 - 2.115 GeV) due to an ambiguous assignment of  $K^+K^-$  combinations to a given  $\phi$ . For completeness, all

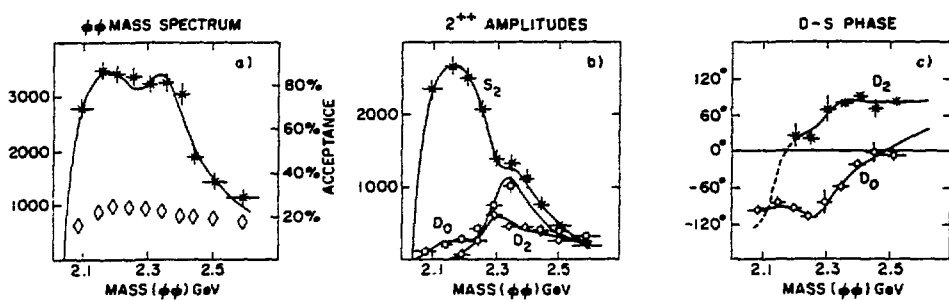


Fig. 11 (a) The acceptance corrected  $\phi\phi$  mass spectrum, (b) intensity and (c) phase difference for the three  $J^{PC} = 2^{++}$  waves. The curves show the fit by three Breit-Wigner resonances (i.e. K-matrix poles). The resonance behavior and parameters are insensitive to the detailed shape of the mass spectrum, and are primarily determined by the six angular distributions and their correlations.

waves with  $J = 0-6$ ,  $L = 0-4$ ,  $S = 0-2$ ,  $P = \pm$  and  $n = \pm$  were included in the partial wave analysis. This amounts to 114  $\phi\phi$  waves to be considered. In our latest work, we improved the analysis by simultaneously doing the partial wave analyses on  $\phi\phi$  and  $\phi K^+K^-$  (the small physical identified background) using up to  $J = 2$  (27  $\phi K^+K^-$  waves).

In an elaborate search for  $\phi\phi$  waves which best describe the data we started out from a two-wave fit. We cycled through all possible combinations of two waves in each of the ten mass bins and requiring continuity of the solution. This procedure was repeated for the three-wave fit once all the two-wave fits were cycled. Fitting with four waves did not improve the likelihood values significantly. The result of all these fits shows that the best and only acceptable fit requires three waves, namely  $J^P_{LSM} = 2^+S20^-$ ,  $2^+D20^-$ , and  $2^+D00^-$  referred to as S2, D2 and D0 respectively which are shown in Fig. 11b. The phases relative to the S here are shown in Fig. 11c. These will be discussed later. A two-wave fit was rejected by  $> 20\sigma$ . Any other three-wave fit was rejected by  $> 13\sigma$ .

The partial wave analysis solution is primarily determined by the angular distributions and correlations of the six angles specifying an event, and these angular distributions and correlations are very insensitive to the details of the acceptance and the detailed shape of the mass spectrum. The expected distributions in the angular variables for various pure spin states with  $J_z = 0$  in the resonant system are shown in Fig. 12a-b. It is clear from these distributions that each pure state is characterized by a highly unique set of signatures mutually exclusive from each other. The most important variables selecting the  $2^+$  states are  $\alpha$ ,  $\alpha_1 - \alpha_2$ , and  $\alpha_1 + \alpha_2$ . Monte Carlo studies indicate that the shape of these distributions are very insensitive to the apparatus acceptance, unlike the Gottfried-Jackson polar angle ( $\beta$ ), for example, which is very dependent on details of the acceptance. A comparison based on projecting the data into 900 fine bins gives a good fit. Figure 12c shows examples of this binning in three representative mass regions.

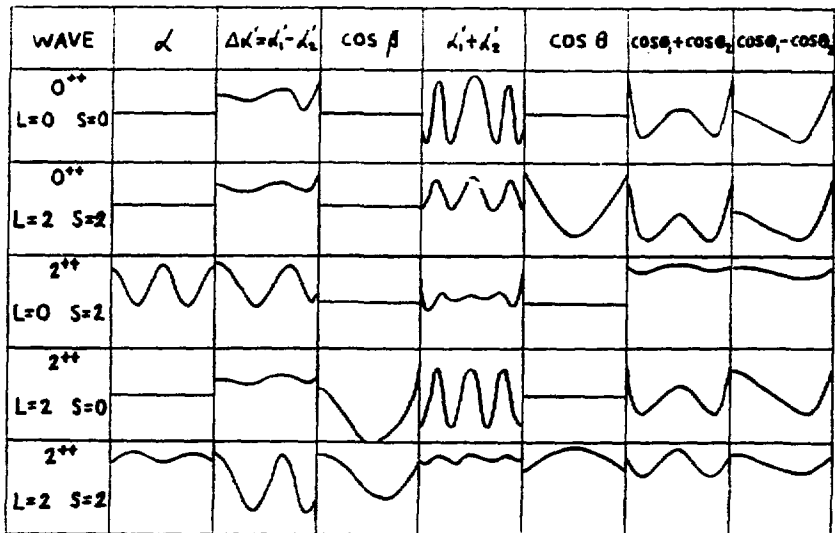


Fig. 12a Various pure waves from  $J^{PC} = 0^{++}$  to  $J^{PC} = 2^{++}$  with  $M = 0$ .

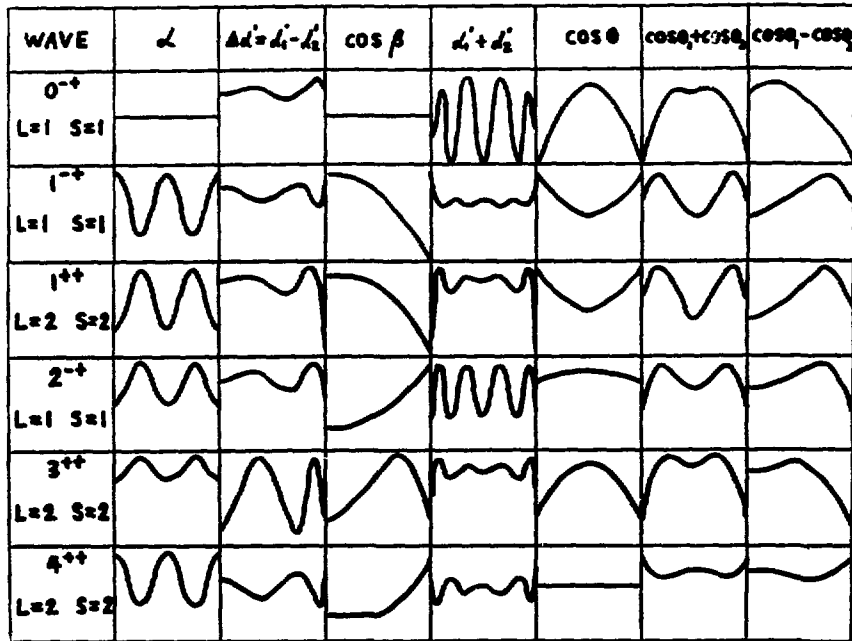


Fig. 12b Various pure waves from  $J^{PC} = 0^{-+}$  to  $J^{PC} = 4^{++}$  with  $M = 0$ .

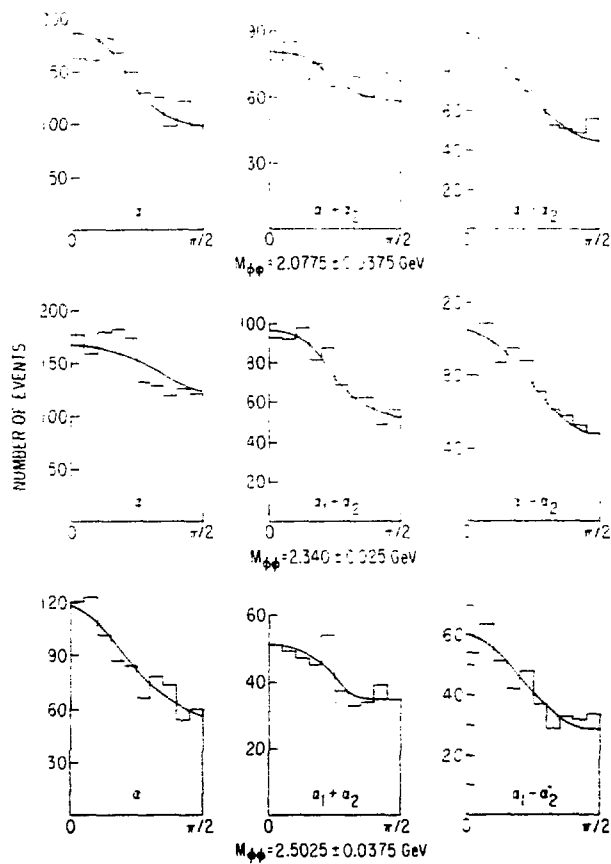


Fig. 12c Angular distributions for  $\alpha$ ,  $\alpha_1 + \alpha_2$ ,  $\alpha_1 - \alpha_2$  in three of the ten mass bins. The  $\pm$  numbers shown on the  $M_{\phi\phi}$  mass values give the half bin size in which the data is grouped. The curves are the three-wave fit modified by the experimental acceptance.

Note that there is a high degree of symmetry and periodicity for angular distributions associated with the  $\phi\phi$  system. We have folded our data to take advantage of these.

All the three required waves have  $J_z = 0$  in the Gottfried-Jackson frame and the exchange naturality =  $(-1)$ , the characteristics of pion exchange. Also, for  $|t'| < 0.3$ , the observed  $(d\sigma/dt')_{\phi\phi} = \exp(-9.50 \pm 0.10) |t'|$  (Fig. 13) again corresponding to

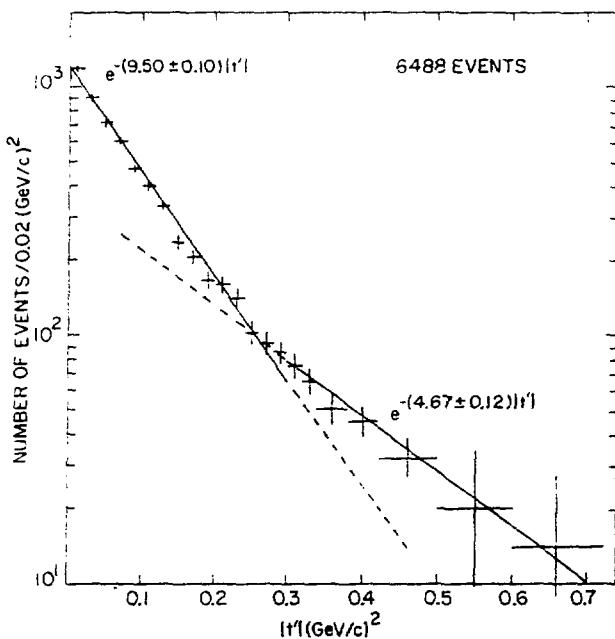


Fig. 13  $\log (\text{const.} \times d\sigma/dt')$  plotted versus  $|t'|$ .

pion exchange. Thus the production mechanism is via  $\pi$ -exchange which accounts for 95% of the  $\phi\phi$  data. For  $|t'| > 0.3$  the slope decreases indicating other exchanges enter.

The points shown in Fig. 11b represent the mass independent determination of these three partial wave amplitudes. The corresponding phase behavior of D0 and D2, measured relative to S2, is shown in Fig. 11c. It is clear from these figures that around 2.3 GeV both D0 and D2 show typical amplitude and phase behavior corresponding to resonances while the behavior of the S2 amplitude suggests a resonance near threshold (~ 2 GeV).

The resonant behaviors of the three  $2^{++}$  states can be further demonstrated by the Argand plots. Since  $1^{--} \pi^+ K^-$  and  $\phi\phi 2^{++}$  are coherent as shown by interference, the  $1^{--}$  phase can be measured relative to the large S2  $\phi\phi$  wave phase and be used as a reference wave for the  $\phi\phi$  waves. In order to assure ourselves that the phases and

amplitudes for  $S_2$ ,  $D_2$ , and  $D_0$  derived from  $1^{--}$  are insensitive to the production mechanism of the  $1^{--}$ , we have studied two extreme cases. In one case the  $1^{--}$  was assumed to have a K-matrix pole which led to a maximum phase traversal of  $340^\circ$ . In another case the  $1^{--}$  was assumed to be produced from a Reggeized multiperipheral Deck mechanism which led to a minimum phase traversal of  $31^\circ$ . The  $1^{--}$  Argand plots for these two cases show different shapes. If  $1^{--}$  has a K-matrix pole the plot looks like a circle while in the Reggeized Deck model it looks like a sausage. The  $1^{--}$  phases measured against the  $S_2$   $2^{++}$   $\phi\phi$  amplitudes corresponding to these two situations are displayed in Fig. 14b.

The resultant Argand plots for each  $\phi\phi$  wave under both conditions of  $1^{--}$  absolute phase are shown in Figs. 14a and 14c. Both extreme cases gave similar classic Breit-Wigner three resonance behavior in amplitude phase and speed behavior near resonance. Thus the actual case which is expected to be somewhere in between these two extremes should also show Breit-Wigner resonance behavior for all three resonances.

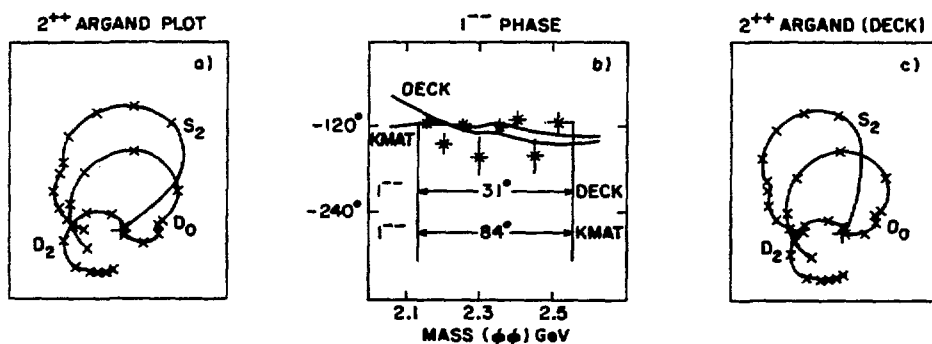


Fig. 14 (a) Argand plots for the three  $2^{++}$  waves with the absolute phase based on the  $1^{--}$   $\phi\phi$  wave being a Breit-Wigner resonance (K-matrix), while (c) is based on the  $1^{--}$   $\phi\phi$  resulting from a deck mechanism. (b) shows the  $1^{--}$  phase (relative to the S-wave in  $\phi\phi$ ). The curves come from the two models stated for the  $1^{--}$  absolute phase.

We used a unitary K-matrix formalism to fit the partial wave analysis.

We fitted the three sets of partial wave amplitudes in ten mass bins. Each pole was allowed to have mixing of all three waves. In order to obtain a good fit we needed three K-matrix poles. In Figs. 11a-c the smooth curves are derived from the three pole K-matrix fit. Two poles gave an unacceptable fit ( $>18\sigma$ ) and a fourth pole did not improve the fit significantly.

It should be noted that each K-matrix pole in our fit corresponds uniquely to an S (or T) matrix pole and thus one can extract the Breit-Wigner resonance parameters corresponding to those poles. These parameters are shown in Table 1. We found unitary effects to be small thus fitting with three complex Breit-Wigner's would give consistent numbers.

Table 1

Parameters of the Breit-Wigner resonances (corresponding to the K-matrix poles) and percentage of the resonances going into  $2^{++}$   $S2$ ,  $D2$ , and  $D0$  channels.

State	$\phi\phi$ Data	Mass(GeV)	Width(GeV)	$S2(\%)$	$D2(\%)$	$D0(\%)$
$g_T$	45%	$2.011^{+.062}_{-.076}$	$.202^{+.067}_{-.062}$	$98^{+1}_{-3}$	$0^{+1}$	$2^{+2}_{-1}$
$g_{T'}$	20%	$2.297^{+.028}_{-.028}$	$.149^{+.041}_{-.041}$	$6^{+15}_{-5}$	$25^{+18}_{-14}$	$69^{+16}_{-27}$
$g_{T''}$	35%	$2.339^{+.055}_{-.055}$	$.319^{+.081}_{-.069}$	$37^{+19}_{-19}$	$4^{+12}_{-4}$	$59^{+21}_{-19}$

The error estimates are related to correlations caused by considerable mixing of the waves comprising the three resonant states. The errors are derived from a complete study of the  $\chi^2$  surface. We generated surfaces in the K-matrix variables which corresponded to a  $\chi^2$  of  $4\sigma$ . These surfaces enclosed our best solution which was  $\sim 2\sigma$  fit.

It is interesting to note that the three  $J\Gamma$  states have typical hadronic widths. In hadrons, the hadronization process is expected to take place near the outer region of confinement involving strongly interacting soft glue, including collective interactions, and this leads to resonance decay with typical hadronic widths. From the glueball physics point of view, a glueball is a collection of strongly coupled gluons with glue-glue coupling being comparable to the quark-glue coupling. Thus it would be expected that glueballs, via gluon splittings before final hadronization and collective interactions, have a similar hadronization process to  $q\bar{q}$  hadrons. Therefore a glueball is expected to have  $\sim$  normal hadronic widths. However, as for oddballs<sup>17)</sup> (glueballs with exotic  $JPC$ ) those widths could be narrow since the underlying cause of suppression of the exotic sector remains unclear.

The constituent gluon model would predict three low-lying  $JPC = 2^{++}$  glueballs. The calculations carried out in the strong coupling limit<sup>18)</sup> have shown three  $J = 2$  glueballs.

A partial wave analysis of the  $\phi K^+ K^- n$  background (Fig. 15) in the region of  $K^+ K^-$  mass just above the  $\phi$  revealed that 67% of it was structureless and incoherent. Approximately 3% of the background was  $JPC = 2^{++}$  which has practically zero amplitudes near the threshold region and peaked at 2.4 GeV with essentially no phase motion. Thus it was totally different than the  $2^{++}$  observed in the  $\phi\phi$  system. There was an additional contribution of 30% of  $JPC = 1^{--}$  in the background, which has expected quantum numbers for a  $\phi K^+ K^-$  system produced by pion exchange with all particles in an S-wave with respect to each other. The  $1^{--}$  is coherent and also produced by  $\pi$ -exchange, therefore this wave interfered with the  $\phi\phi$   $2^{++}$  amplitudes. The smooth curves for the  $1^{--}$  and  $2^{++}$  in Fig. 15 are Breit-Wigner fits with just one pole for each wave.

#### GLUEBALL INTERPRETATION

The preceding results for the reaction  $\pi^- p \rightarrow \phi \bar{n}$  have shown unusual and striking characteristics which have not been observed in other uds hadronic reactions. In fact, these observations point to the

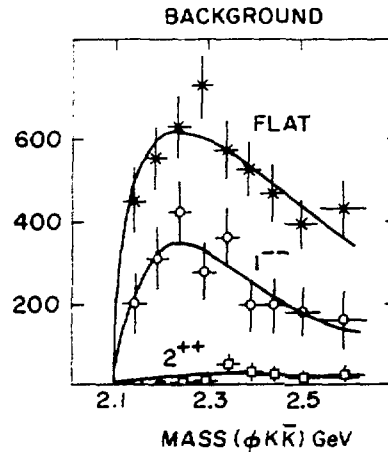


Fig. 15 Intensity of the partial waves in the background reaction  $\pi^-p \rightarrow \phi K^+K^-n$ . The smooth curves are Breit-Wigner fits for the  $1^{--}$  and  $2^{++}$ , where the flat in all angular variables background fit is an exponent times the threshold factor.

need for a new phenomenon in order that these characteristics can be satisfactorily accounted for. The following observations are especially relevant:

In a partial wave analysis and an unitary K-matrix fit we found that the production of  $\phi\phi$  is via  $\pi$ -exchange and the expected suppression due to this disconnected process is completely broken. It has been further demonstrated that the OZI violating amplitudes of  $\pi\pi$  annihilation going into  $\phi\phi$  can be totally described by three required resonance states, all with the same quantum numbers  $I^GJ^P = 0^+2^{++}$ , and no continuum or other states (within errors). In contrast, the OZI-allowed background process  $\pi^-p \rightarrow \phi K^+K^-n$ , which is mostly structureless, accounts only for a few percent of the  $\phi\phi$  production. The contribution coming from another OZI-allowed background reaction  $\pi^-p \rightarrow K^+K^-K^+K^-n$  is almost negligible (0.1%). The  $I^GJ^P = 0^+4^{++}$   $h(2040)$  has strong  $\pi\pi$  coupling, the absence of a detectable  $h$ -meson signal in the  $\phi\phi$  channel provides independent evidence for the selectivity of the  $2^{++}$  quantum numbers and the filtering action of the

OZI rule observed in this channel. In another hadronic reaction  $\phi\phi \rightarrow K_S^0 K_S^0 n$  also at 22 GeV/c,<sup>19)</sup> which is both OZI-allowed and produced by  $\pi$ -exchange, each amplitude corresponding to  $0^{++}$ ,  $2^{++}$  and  $4^{++}$  in the same range 2.0 - 2.5 GeV was measured to be populated. The slowly varying non-resonant  $2^{++}$  amplitudes with clear absence of phase motion again reinforce the preceding conclusions.

Both the  $\phi\phi$  and  $\phi K^+ K^-$  events were simultaneously partial wave analyzed. It is clear that these two reactions show completely different physical behaviors. The  $\phi K^+ K^-$  background reaction is mostly (67%) featureless and incoherent, and has flat angular distributions. About 30% is  $1^{--}$  whose presence in the  $\phi K^+ K^-$  can be attributed to a kinematic effect of a three-body system. Only 3% of the entire  $\phi K^+ K^-$  events is  $2^{++}$  with vanishing amplitudes near the  $\phi\phi$  threshold, peaks beyond the three  $g_T$  states, and practically has no phase motion. Thus the characteristics of the OZI-allowed and OZI-forbidden processes with approximately the same threshold are remarkably different. It is apparent that the  $g_T$ ,  $g_T'$  and  $g_T''$  can hardly be produced by a naive threshold mechanism.

These very striking phenomena are naturally explained in the context of QCD if one assumes 1-3 primary glueballs with  $J^{PC} = 2^{++}$  produce these states.<sup>5,20-21)</sup> At least one primary glueball is required to break the OZI suppression and select only  $J^{PC} = 2^{++}$  resonant states. It could then mix with one or two other conventional  $q\bar{q}$  states. Of course, the simplest explanation is that we have found a triplet of  $J^{PC} = 2^{++}$  glueballs.

Alternative explanations which have been proposed to explain the  $\phi\phi$  data without the need of a glueball were found to be either incorrect or did not fit the unusual characteristics of our data.<sup>5</sup> In fact, there is no other than a glueball explanation so far why in  $\phi\phi$  we see three closely spaced isosinglet  $J^{PC} = 2^{++}$  resonances, and nothing else whereas in  $\phi K^+ K^-$  and  $K_S^0 K_S^0 n$  we see virtually all non-resonant background and no evidence of resonances.

## CONCLUSION

In conclusion, in our partial wave analysis of the reaction  $\pi^- p \rightarrow \phi \bar{\phi} n$  using 6658 events we have observed three resonance states, the  $g_T$ ,  $g_T'$  and  $g_T''$  all with  $J^{PC} = 2^{++}$ ,  $M\eta = 0^-$ . These three resonances virtually comprise all the cross section of that reaction. Using the coherent  $1^{--}$  wave from the  $\pi^+ K^-$  background as the phase reference for the three  $\phi\phi$  dominant waves  $S2$ ,  $D2$  and  $D0$  the classic amplitude and phase resonance behavior of  $g_T$ ,  $g_T'$  and  $g_T''$  are clearly demonstrated. There is striking evidence for the breakdown of the OZI rule in this reaction. The production mechanism is via  $\pi$ -exchange. Within the context of QCD the unusual features of the data and the production of the  $g_T$ ,  $g_T'$  and  $g_T''$  can be well explained as annihilation of the valence quarks in a  $\pi^+ \pi^-$  pair into resonating gluons which break down the OZI suppression very selectively. The resonances observed can be explained by assuming that 1-3 primary glueballs with  $J^{PC} = 2^{++}$  produce these states. At least one glueball is necessary to explain the selective breakdown of the OZI suppression and the strong filtering which led to the absence of other states such as  $h(2040)$  and background found in other experiments.

After a review<sup>3)</sup> of the other glueball candidates it becomes clear that among a variety of glueball candidates, that the three  $g_T$ ,  $g_T'$ ,  $g_T''$  states constitute the only strong glueball candidates. Their unique characteristics can be naturally explained within the context of QCD by the production of 1-3  $J^{PC} = 2^{++}$  primary glueballs. No other interpretation which is correct and fits the data has survived. On the other hand the other glueball candidates do not have any compelling argument for being a glueball.

## FORTHCOMING EXPERIMENT (SEARCH FOR EXOTIC GLUEBALLS)

As part of the plan in our continued effort in glueball studies, our next objective for the forthcoming experiment is to search for oddballs, or glueballs with exotic quantum numbers.

However, it is clear from  $d\sigma/dt'$  plot (Fig. 17) and  $M^2 = 0^-$  for the three required waves S2, D0 and D2, for  $|t'| < 0.3$  (95% of the data) the production of  $\phi\phi$  is dominated by  $\pi$ -exchange and thus only  $jPC = 0^{++}, 2^{++}, 4^{++} \dots$  etc. can be produced. In order to produce exotic states such as  $1^{-+}$  etc. A or other exchanges are required. The exchanges other than pion are expected to take place when the slope of the  $d\sigma/dt'$  plot changes from  $\sim 10$  to  $\sim 5$  for  $|t'| > 0.3$ . In a phenomenological study, we have found that by lowering down the incident momentum to 8 GeV/c from the present 22 GeV/c and also optimizing our experimental setup it is possible to achieve a factor of 8 increase in high  $|t'| (> 0.3)$  data acquisition over the same running period while still maintaining the overall acceptance.

## REFERENCES

1. a) Fritzsch and Minkowski, *Nuovo Cimento* 30A, 393(1975).  
 b) R.P. Freund and Y. Nambu, *Phys. Rev. Lett.* 34, 1645(1975).  
 c) R. Jaffee and K. Johnson, *Phys. Lett.* 60B, 201 (1976).  
 d) Kogut, Sinclair and Susskind, *Nucl. Phys.* B114, 199 (1975).  
 e) J. Bjorken, SLAC Pub. 2372.
2. a) C. Michael and I. Teasdale, *Glueballs From Asymmetric Lattices*, Liverpool Univ. Preprint LTH-127, March 1985.  
 b) Ph. De Forcrand *et al.*, *Phys. Lett.* 152B, 107 (1985).  
 c) S.W. Otto and P. Stolorz, *Phys. Lett.* 151B, 428 (1985).  
 d) G. Schierholz and M. Teper, *Phys. Lett.* 136B 64 (1984).  
 e) Bernd Berg, *The Spectrum in Lattice Gauge Theories*, DESY Preprint 84-012, Feb. 1984.
3. S.J. Lindenbaum, "A Review of Experimental Progress in Gluonia," *Proc. of the XXIV Intern. Conf. on High Energy Physics, Munich, West Germany, August 4-11, 1988* (to be published).
4. a) A. Etkin *et al.*, *Phys. Rev. Lett.* 40, 422 (1978); 41, 784 (1978); 49, 1620 (1982); *Phys. Lett.* B165 217 (1985);  
 b) A. Etkin *et al.*, *Phys. Lett.* B201, 568 (1988).
5. S.J. Lindenbaum, *Superstrings, Supergravity, and Unified Theories*, The ICTP Series in Theoretical Physics, Vol. 2 (World Scientific, Singapore, 1986) pp. 548-593; S.J. Lindenbaum and R.S. Longacre, *Phys. Lett.* 165B, 202 (1985).
6. Edwards *et al.*, *Phys. Rev. Lett.* 48, 458 (1982).
7. Longacre *et al.*, *Phys. Lett.* 177B, 223 (1986).

REFERENCES (continued)

8. T. Bolton, MK III Thesis, MIT, April 1988.
9. Etkin et al., Phys. Rev. D25, 2446 (1982); Phys. Rev. D25, 1786 (1986); Sosnovsky et al., Proc. Intern. Europhysics Conf. on High Energy Physics, Uppsala, June 25-July 1, 1987, p. 558.
10. Alde et al., Nuc. Phys. B269, 485 (1986).
11. S.J. Lindenbaum and R.S. Longacre (to be published).
12. P.S. Booth et al., Nuc. Phys. B273 (1980); 687 and 689.
13. Particle Data Group Tables, 1986 and 1988.
14. T. Armstrong et al., Phys. Letts. B121, 83 (1983).
15. M. Baubillier et al., Phys. Lett. B118 (1982) 450.
16. S.J. Lindenbaum, Il Nuovo Cimento 65A, 222-238 (1981)
17. a) S. Meshkov, Proc. of the Seventh Intern. Conf. on Experimental Meson Spectroscopy, April 14-16, 1983, Brookhaven National Laboratory, S.J. Lindenbaum, Editor, AIP Conf. Proc. No. 113, p. 125-156.  
b) P.M. Fishbane and S. Meshkov, Comment on Nuclear and Particle Physics 13, 325 (1984).
18. T.D. Lee, "Time as a Dynamical Variable," CU-TP-266, Talk at Shelter Island II Conf., June 2, 1983.
19. a) R.S. Longacre et al., Talk presented at The 2nd International Conf. on Hadron Spectroscopy, KEK, Tsukuba, Japan, April 16-18, 1987; BNL Preprint 39953.  
b) R.S. Longacre et al., Talk presented at Proc. of the 23rd Intern. Conf. on High Energy Physics, Sept. 24, 1986; BNL Preprint 38729.  
c) A. Etkin et al., Phys. Rev. D25, 1786-1802 (1982).
20. a) S.J. Lindenbaum, Hadronic Production of Glueballs. Proc. 1983 Intern. Europhysics Conf. on High Energy Physics, Brighton, U.K., July 20-27, 1983, J. Guy and C. Constatin, Editors (Rutherford Appleton Laboratory), p. 351-360.  
b) S.J. Lindenbaum, Production of Glueballs. Comments on Nuclear and Particle Physics 13, #6, 285-311 (1984).  
c) S.J. Lindenbaum, The Glueballs of QCD and Beyond. Invited Lecture. Proc. 22nd Course of the International School of Subnuclear Physics on "Quarks, Leptons and their Constituents," Erice, Trapani-Sicily, Italy, 5-15 August 1984.

REFERENCES (continued)

21. S.J. Lindenbaum, Talk presented at the 3rd Conf. on the Interactions between Particle and Nuclear Physics, May 14-19, 1988, Rockport, Maine.
22. Novikov et al., Nucl. Phys. B191, 301 (1981).